

## Contraction-Driven Cell Motility

P. Recho,\* T. Putelat, and L. Truskinovsky

*LMS, CNRS-UMR 7649, Ecole Polytechnique, Route de Saclay, 91128 Palaiseau, France*

(Received 21 December 2012; published 5 September 2013)

We propose a mechanism for the initiation of cell motility that is based on myosin-induced contraction and does not require actin polymerization. The translocation of a cell is induced by symmetry breaking of the motor-driven flow, and the ensuing asymmetry gives rise to a steady motion of the center of mass of a cell. The predictions of the model are consistent with observations on keratocytes.

DOI: [10.1103/PhysRevLett.111.108102](https://doi.org/10.1103/PhysRevLett.111.108102)

PACS numbers: 87.16.Uv, 87.10.Ca, 87.16.Ln, 89.75.Kd

Structural rearrangements allowing cells to crawl on substrates (e.g., keratocytes or fibroblasts) involve spatial and temporal self-organization at the level of cytoskeleton—a dynamic protein network inside the cell combining the functions of support and driving [1]. To reach motile configuration, a cell must first polarize, which implies loss of circular symmetry, decentering of the nucleus, and regroupment of myosin motors at the trailing edge. The fact that such symmetry-breaking internal instabilities, leading to steady self-propulsion, have been observed even in nucleus-free fragments [2] suggests that the underlying mechanism has a relatively simple origin, and several models emphasizing different physics have been recently proposed in the literature [3–7].

The three major processes responsible for cell motility are protrusion, contraction, and adhesion [1]. They are all induced by ATP hydrolysis: protrusion is caused by polymerization and depolymerization of actin filaments, contraction results from the activity of myosin motors, and adhesion is mediated by engagement and disengagement of transmembrane receptors. For cells, crawling on rigid substrates, the ATP dependence of adhesion can be neglected and the associated interaction is often treated as passive [8–10]. Both myosin contraction and actin polymerization contribute to cell migration as active, ATP-driven mechanisms; however, their roles appear to be complementary [10]. In particular, contraction is believed to be solely responsible for cell polarization [2]. Furthermore, experimental studies of epithelial tumors [11] strongly suggest that at least some cells can be driven exclusively by contraction.

To explain these experiments, we propose a simple model showing the possibility of spontaneous polarization and self-propulsion without ATP-driven protrusion, which is a crucial component of many recent models [6,12]. We argue that the *positive* feedback mechanism, giving rise to the symmetry-breaking instability of a nonmotile configuration and ensuring directional motility of a self-propelling cell, is similar to an uphill diffusion. It is driven by advection of molecular motors that in turn mechanically propel the actin network by inflicting contraction and creating an autocatalytic effect [13]. The coupling leads to build up of

local motor concentration, which is limited by elasticity, friction, and diffusion, resisting the runaway and providing the *negative* feedback.

The idea that contraction causes flow which in turn carries the regulators of contraction is incorporated into the hydrodynamic description of active fluids [14]. In configurations with fixed boundaries, it has been shown to describe instabilities leading to nontrivial *symmetric* patterns of stress activator [5]. In Ref. [7], similar ideas were used in the description of nonlamellipodial motility associated with angular cortex flows. Heuristic models of the Keller-Segel type [15] describing polarization instability in static cells were proposed in Refs. [16,17]. In all these papers, however, the effect of myosin-induced contraction was either obscured by the account of other symmetry-breaking mechanisms, in particular, actin treadmilling, or the focus was on generation of internal flow rather than on the translocation of the center of mass of a cell. There also exists considerable literature addressing spontaneous motility driven directly by protrusion [3] and Turing patterning [18] or studying an interplay of multiple mechanisms [19,20].

Recently, a model of contraction-induced motility relying on splay instability was proposed in Ref. [4]. This mechanism is complementary to *autotaxis* studied in the present Letter. Lately, the contraction-induced motility initiation was attributed to an instability in a poro-elastic active gel permeated by a solvent [21]. The implied mechanism is conceptually close to autotaxis, but other physical factors are involved as well.

To make the physics of contraction-dominated motility fully transparent, we study in this Letter an analytically tractable one-dimensional model that captures both the symmetry breaking and the induced macroscopic motion in the minimal setting. We show that an increase of motor concentration beyond a threshold leads to a bifurcation from a static symmetric regime to an asymmetric motile regime describing a self-propelling cell. While several static and dynamic steady regimes may be available for the same value of parameters, we show that only the motile solution localizing motors near the *trailing edge* of the cell is stable, which is in agreement with observations [2].

*The model.*—Consider the force balance equation for a one-dimensional layer of an active gel in viscous contact with a rigid background  $\partial_x \sigma = \xi v$ , where  $\sigma(x, t)$  is the stress,  $v(x, t)$  is the velocity of the acto-myosin network, and  $\xi$  is the friction coefficient. Following Refs. [5,9,22], we write  $\sigma = \eta \partial_x v + \chi c$ , where  $\eta$  is the bulk viscosity,  $c$  is the concentration of motors, and  $\chi > 0$  is the contractile active stress (per motor). The function  $c(x, t)$  satisfies the advection-diffusion equation  $\partial_t c + \partial_x (cv) = D \partial_{xx} c$ , where  $D$  is the diffusion coefficient. We assume that  $l_-(t)$  and  $l_+(t)$  are the unknown boundaries of the cell. We account for a mean field-type linear elastic interaction due to membrane or cortex [23] by using mechanical boundary condition  $\sigma(l_{\pm}(t), t) = -k(L - L_0)/L_0$ , where  $L(t) = l_+(t) - l_-(t)$  is the length of the cell,  $k$  is the effective elastic stiffness, and  $L_0$  is the reference length. Since we neglect active treadmilling, we can write the kinematic boundary conditions in the form  $\dot{l}_{\pm} = v(l_{\pm})$ . We impose zero exterior flux of motors  $\partial_x c(l_{\pm}(t), t) = 0$ , which implies that the average concentration  $c_0 = L_0^{-1} \int_{l_-}^{l_+} c(x, t) dx$  is conserved.

If we now normalize length by  $L_0$ , time by  $L_0^2/D$ , concentration by  $c_0$ , and stress by  $k$ , we obtain a Keller-Segel-type system [24]

$$-Z \partial_{xx} \sigma + \sigma = \mathcal{P} c, \quad \partial_t c + \mathcal{K} \partial_x (c \partial_x \sigma) = \partial_{xx} c, \quad (1)$$

where the dimensionless constants are  $Z = \eta/(\xi L_0^2)$ , comparing our two frictional mechanisms,  $\mathcal{K} = k/(\xi D)$ , measuring relative importance of diffusion, and  $\mathcal{P} = c_0 \chi/k$ , giving the scale of contractile activity. If  $\sigma$  is expressed through the corresponding Green's function, the resulting nonlocal diffusion-advection problem is structurally similar to the one proposed in Ref. [16]; however, the effective kernel is different. Conceptually, the proposed motility mechanism is similar to chemotaxis [15] but in a purely mechanical setting.

The dimensionless boundary conditions for Eq. (1) take the form  $\sigma(l_{\pm}(t), t) = -(L(t) - 1)$ ,  $\partial_x c(l_{\pm}(t), t) = 0$ , and  $\dot{l}_{\pm}(t) = \mathcal{K} \partial_x \sigma(l_{\pm}(t), t)$ . They imply that the motion of the center of the cell  $G(t) = (l_-(t) + l_+(t))/2$  is governed by the equation

$$\dot{G}(t) = \frac{\mathcal{K} \mathcal{P}}{2Z} \int_{l_-(t)}^{l_+(t)} \frac{\sinh[(G-x)/\sqrt{Z}]}{\sinh[L/(2\sqrt{Z})]} c(x, t) dx. \quad (2)$$

If the concentration distribution is symmetric, then  $\dot{G} = 0$  and the cell cannot move, which is a simple analogue of Purcell's theorem [25] with spatial asymmetry required for steady self-propulsion replacing temporal asymmetry of a periodic stroke. From Eq. (2) we also infer that the maximal speed of the cell is equal to  $\mathcal{K} \mathcal{P}/(2Z)$ . In dimensional variables [5,9], this gives  $\chi L_0 c_0/(2\eta) \approx 10 \mu\text{m}/\text{min}$ , which is realistic [2].

*Steadily advancing cells.*—In a steady motility mode, both stress and myosin concentration must depend only on traveling wave coordinate  $y = x - Vt$  where  $V$  is the

unknown cell velocity. We also have  $\dot{l}_{\pm} = V$  and  $L(t) = L$  where  $L$  is the unknown length of the cell. Then system Eq. (1) reduces to the single equation

$$-Z s''(y) + s(y) - \mathcal{K}(L - 1) = \mathcal{K} \mathcal{P} \frac{\exp(s(y) - Vy)}{\int_0^L \exp(s(y) - Vy) dy}, \quad (3)$$

where  $s(y) = \mathcal{K}[\sigma(y) + (L - 1)]$  is the unknown function. The presence of four boundary conditions  $s(0) = s(L) = 0$  and  $s'(0) = s'(L) = V$  ensures that both parameters  $V$  and  $L$  can be found along with  $s(y)$ . After Eq. (3) is solved, the motor concentration profile can be recovered from the relation  $c(y) = \exp(s(y) - Vy) [\int_0^L \exp(s(y) - Vy) dy]^{-1}$ . To simplify the description, we assume that  $Z = 1$  [9], which means that the elastic and the viscous scales are correlated. We are then left with two dimensionless parameters  $\mathcal{K} \sim 100$  and  $\mathcal{P} \sim 0.1$  [7,9].

*Initiation of motility.*—Directional motion starts with an instability of a static solution of Eq. (3). All such solutions are necessarily symmetric and can be written in quadratures [5]. In addition to regular static states, there are also singular static states with zero length  $\hat{L}_0 = 0$  and  $s(y) = \lim_{\theta \rightarrow 0} \theta f(y/\theta)$ , where  $f(u) = (\mathcal{K} \mathcal{P}/2)u(1-u)$  and  $u \in [0, 1]$ ; moreover, for  $\mathcal{P} > 1/4$ , those are the only static configurations. Singular (measure valued) solutions of this type have been encountered in several problems leading to Eq. (3) from turbulence to gauge theory [26], and here they describe the collapse of a cell under the action of unbalanced contractile stresses.

One can show that motile branches with  $V \neq 0$  bifurcate only from homogeneous static solutions with  $s(y) = 0$  and

$$\hat{L}_{\pm} = (1 \pm \sqrt{1 - 4\mathcal{P}})/2. \quad (4)$$

Notice that the “rest length” of static cell depends only on the normalized global motor content  $\mathcal{P}$ . Linearization around these states produces the following linear problem for the perturbation  $\delta s(z)$

$$\delta s'' + \omega^2 \delta s = A + Bz, \quad (5)$$

where  $z = y/L$ ,  $A = -(\omega^2 + \hat{L}^2)[(2\hat{L} - 1)/(\hat{L}^3(\hat{L} - 1))\delta L - (1/2)\hat{L}\delta V]$ ,  $B = -\hat{L}(\omega^2 + \hat{L}^2)\delta V$ , and

$$\omega = \sqrt{\mathcal{K} \mathcal{P} \hat{L} - \hat{L}^2}.$$

Equation (5) is supplemented with the four boundary conditions  $\delta s(0) = \delta s(1) = 0$ ,  $\delta s'(0) = \delta s'(1) = \hat{L}\delta V$ , allowing one to find the perturbations of the cell length  $\delta L$  and its speed  $\delta V$  (up to a common multiplier).

Equation (5) has nontrivial solutions if  $\omega \neq 0$  and

$$2\hat{L}^2(\cos \omega - 1) + (\omega^2 + \hat{L}^2)\omega \sin \omega = 0. \quad (6)$$

Solutions of Eq. (6) split into two families. The first family  $S1, S2, \dots$  with  $\omega = 2m\pi$ , where  $m$  is a positive integer, corresponds to static configurations with  $\delta V = 0$ . The

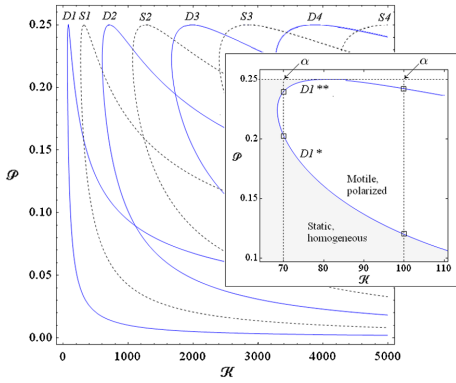


FIG. 1 (color online). Locus of the bifurcation points in the  $(\mathcal{K}, \mathcal{P})$  plane. Inset shows a zoom on the  $D1$  branch around the turning point at  $\mathcal{P} = 1/4$ . The bifurcation diagrams along two sections  $\mathcal{K} = 100$  and  $\mathcal{K} = 70$  are shown in Figs. 2 and 4, respectively.

second family  $D1, D2, \dots$  parametrized by the roots of the equation  $\tan(\omega/2) = \omega/2(1 + \omega^2/\hat{L}^2)$ , corresponds to motile solutions with  $\delta L = 0/2$ . The locus of the bifurcation points in the parameter plane  $(\mathcal{P}, \mathcal{K})$  is shown in Fig. 1. At a given value of  $\mathcal{K}$ , a homogeneous static configuration becomes unstable when the measure of motor activity reaches the threshold  $\mathcal{P} = \mathcal{P}_0$ , which can be found from the equation  $\omega^2 + \hat{L}_+^2(\mathcal{P}_0) = \mathcal{K}\mathcal{P}_0\hat{L}_+(\mathcal{P}_0)$ , where  $\omega(\hat{L}_+(\mathcal{P}_0))$  is the smallest positive root of Eq. (6). Notice that at sufficiently small values of  $\mathcal{K}$ , when either diffusion or friction are too strong, neither polarization nor motility are possible independent of the level of motor activity.

*Nonlinear regimes.*—To follow bifurcated branches into the nonlinear regime, we performed a numerical study of Eq. (3). In Fig. 2, we see that a pitchfork bifurcation at  $D1^*$

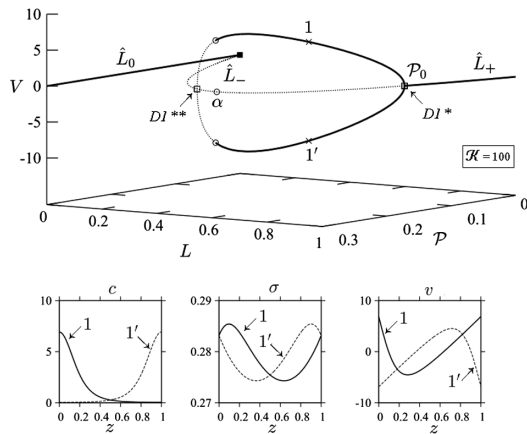


FIG. 2. Bifurcation diagram at  $\mathcal{K} = 100$  showing motile branches connecting bifurcation points  $D1^*$  and  $D1^{**}$  from Fig. 1. Solid lines show stable solutions, and dotted lines correspond to unstable solutions. Three graphs below show the internal profiles at  $\mathcal{P} = 0.2$  corresponding to branch 1 (solid) and branch 1' (dashed).

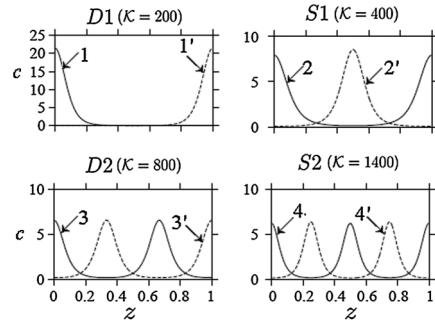


FIG. 3. Inhomogeneous solutions  $D1, S1, D2, S2$  at  $\mathcal{P} = 0.245$ . Even labels (1,3) correspond to asymmetric motile regimes, and odd labels (2,4) correspond to static symmetric regimes. Each static regime is represented by two solutions with larger and smaller lengths, e.g., 2 and 2'.

gives rise to two motile branches reconnecting at  $D1^{**}$ . This bifurcation describes the initiation of motility at  $\mathcal{P} = \mathcal{P}_0$ . The choice of polarization is dictated by imperfections and the resulting motility pattern with motors localizing at the trailing edge (see regimes 1 and 1' in Figs. 2 and 3) is similar to the one observed in experiments carried on keratocyte fragments [2].

Other bifurcation points give rise to either static or motile solutions that always appear in pairs. In particular, static bifurcation associated with  $S1$  leads to two configurations with motors concentrated in either the middle of the cell or near the boundaries (see regimes 2 and 2' in Fig. 3). Along the second motile branch  $D2$ , there is an additional peak in the concentration profile compared to that of  $D1$  (see regimes 3 and 3' in Fig. 3).

In Fig. 4, we illustrate a possibility of reentrant phenomenon that is similar to the behavior reported in Ref. [16] for a different but related system. In this regime, the increase of the average concentration of motors first polarizes the cell and initiates motility, but then, as the concentration is further increased, the cell gets symmetrized again in another static homogeneous configuration.

*Flow of actin.*—By solving Eq. (1), we obtain the concentration of myosin but not the actin density  $\rho(x, t)$ , which decouples due to the assumption of infinite compressibility

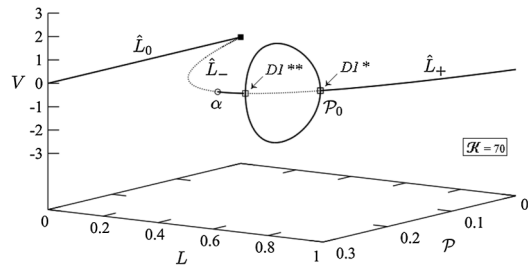


FIG. 4. Bifurcation diagram at  $\mathcal{K} = 70$  illustrating the reentrant behavior; points  $D1^*$  and  $D1^{**}$  are also shown in Fig. 2. Solid lines show stable branches, and dotted lines correspond to unstable branches.

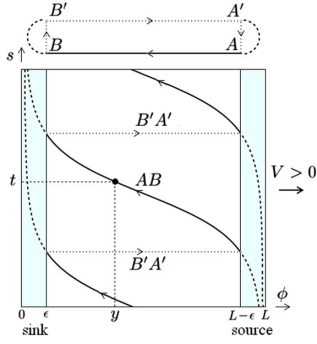


FIG. 5 (color online). Trajectory of an individual actin particle undergoing passive treadmilling for a typical solution on the  $D1$  motile branch with  $V > 0$ . Shaded regions are excluded domains of singular behavior.

[9,20]. To recover the missing information, we have to solve the mass balance equation for actin  $\partial_t \rho + \partial_x(\rho v) = 0$  where the velocity field is given by  $v = \mathcal{K} \partial_x \sigma$ . The structure of solution can be understood by studying the characteristics  $\phi(s)$  of the equation for density [10]. For steady cells moving with velocity  $V$ , we write in the cell's reference frame  $d\phi(s)/ds = v(\phi(s)) - V$ . To ensure that a characteristic passes through the given point  $(y, t)$ , we need to add the boundary condition  $\phi(t) = y$ .

Notice that the points where  $v(y) = V$  are sinks if  $\partial_y v < 0$  and sources if  $\partial_y v > 0$  and it takes infinite time for a characteristic to reach (or to escape from) such singularities. This is clearly a shortcoming of the one-dimensional approach, and to regularize the problem it is natural to cut out small domains of size  $\epsilon$  around singularities; see Fig. 5. We can then represent the “returning” flow, mimicking the three-dimensional circulation, by discontinuities and assume that a particle reaching the boundary of the sink region following a smooth trajectory (path  $AB$  in Fig. 5) instantly reappears on the boundary of the source region (path  $B'A'$  on Fig. 5).

**Transients.**—A numerical study of the initial value problem (1) shows that all nontrivial solutions (static and motile) are unstable except for the branch bifurcating at  $D1$ . Homogeneous solutions from the  $\hat{L}_+$  family and all singular static solutions from the  $\hat{L}_0$  family are numerically stable. In Figs. 2 and 4, stable traveling wave solutions of Eq. (1) are shown with solid lines, and unstable solutions are shown with dotted lines. Simulations also suggest that as in Refs. [5,16], unstable multi-peaked solutions are long lived. This behavior is reminiscent of the classical spinodal decomposition modeled by the Cahn-Hilliard equation where the coarsening process gets critically slowed down near multiple saddle points [27].

**Limiting regimes.**—In some special cases, our equations can be simplified; however, the solutions become more singular. Thus, in the hyperbolic limit  $\mathcal{K} \rightarrow \infty$  (weak diffusion), the number of bifurcation points grows to infinity (see Fig. 1) and solutions become measure valued. As

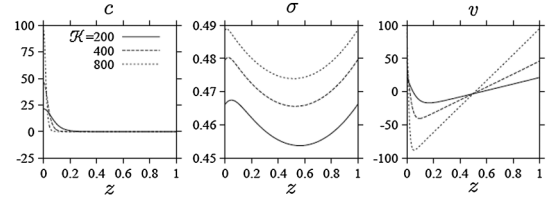


FIG. 6. Internal configurations for the motile branch  $D1$  with  $V > 0$  at  $\mathcal{P} = 0.245$  and increasing  $\mathcal{K}$  value.

an illustration, we show in Fig. 6 the concentration profile for the first motile branch  $D1$ , which infinitely localizes at the trailing edge as  $\mathcal{K} \rightarrow \infty$ .

In the inviscid limit  $Z \rightarrow 0$ , the system (1) reduces to  $\partial_t u = \partial_x(u \partial_x u)$ , where  $u = 1 - \mathcal{K} \mathcal{P} c$ . This is a degenerate sign-indefinite porous flow equation exhibiting an uphill diffusion when  $c > (\mathcal{K} \mathcal{P})^{-1}$ .

To study a cell with a fixed length, we need to assume that  $k \rightarrow \infty$ . This can be interpreted as the double limit  $\mathcal{K} \rightarrow \infty$  and  $\mathcal{P} \rightarrow 0$ . It is then convenient to restore  $Z$  and use as a second dimensionless parameter the product  $\mathcal{K} \mathcal{P}$ . In this limit, the length of the cell is set  $L \rightarrow 1$ ; however, the cell can still move with  $V \neq 0$ . The analysis, similar to the one in the general case, shows that at a sufficiently large value of  $\mathcal{K} \mathcal{P}$  the homogeneous solution with  $V = 0$  becomes unstable. As a result, the macroscopically “rigid” cell internally polarizes and starts to move. Therefore, if a cell with fixed length is allowed to move, all symmetric inhomogeneous configurations with  $V = 0$  studied in Ref. [5] are unstable.

**Conclusions.**—We proposed a prototypical model of a crawling cell showing the possibility of spontaneous polarization and steady self-propulsion in the conditions when contraction is the only active process. This model complements the existing theories of polarization, which place emphasis on the ATP-driven polymerization of actin. Mathematically, the problem reduces to a Keller-Segel-type system with nonlocality due to mechanical rather than chemical feedback. The peculiar nature of the resulting problem is the presence of free boundaries that destabilize symmetric patterns characteristic for active gels in fixed domains. We have shown that the spontaneous symmetry breaking takes place at a critical value of the average concentration of motors and that among the variety of motile regimes describing self-propelling active bodies with internal segmentation, only the simplest polarized configurations observed in experiments are stable.

The authors thank J.F. Joanny, K. Kruse, and A. Mogilner for helpful comments. The work of P.R. was supported by the Monge Doctoral Fellowship from Ecole Polytechnique.

\*pierre.recho@curie.fr

[1] B. Alberts *et al.*, *Molecular Biology of the Cell* (Garland Science, New York, 2002); D. Bray, *Cell Movements*

- (Garland Science, New York, 2000); A. Mogilner, J. Allard, and R. Wollman, *Science* **336**, 175 (2012).
- [2] A. B. Verkhovskiy, T. M. Svitkina, and G. G. Borisy, *Curr. Biol.* **9**, 11 (1999); G. Csucs, K. Quirin, and G. Danuser, *Cell Motil. Cytoskeleton* **64**, 856 (2007); M. L. Lombardi, D. A. Knecht, M. Dembo, and J. Lee, *J. Cell Sci.* **120**, 1624 (2007); P. T. Yam, C. A. Wilson, L. Ji, B. Hebert, E. L. Barnhart, N. A. Dye, P. W. Wiseman, G. Danuser, and J. A. Theriot, *J. Cell Biol.* **178**, 1207 (2007); M. Vicente-Manzanares, X. Ma, R. S. Adelstein, and A. R. Horwitz, *Nat. Rev. Mol. Cell Biol.* **10**, 778 (2009); R. Poincloux, O. Collin, F. Lizarraga, M. Romao, M. Debray, M. Piel, and P. Chavrier *Proc. Natl. Acad. Sci. U.S.A.* **108**, 1943 (2011).
- [3] A. C. Callan-Jones, J. F. Joanny, and J. Prost, *Phys. Rev. Lett.* **100**, 258106 (2008); K. Doubrovinski and K. Kruse, *Phys. Rev. Lett.* **107**, 258103 (2011).
- [4] E. Tjhung, D. Marenduzzo, and M. E. Cates, *Proc. Natl. Acad. Sci. U.S.A.* **109**, 12381 (2012).
- [5] J. S. Bois, F. Jülicher, and S. W. Grill, *Phys. Rev. Lett.* **106**, 028103 (2011); J. Howard, S. W. Grill, and J. S. Bois, *Nat. Rev. Mol. Cell Biol.* **12**, 392 (2011).
- [6] F. Ziebert and I. S. Aranson, *PLoS One* **8**, e64511 (2013).
- [7] R. J. Hawkins, O. Bénichou, M. Piel, and R. Voituriez, *Phys. Rev. E* **80**, 040903(R) (2009); R. J. Hawkins, R. Poincloux, O. Bénichou, M. Piel, P. Chavrier, and R. Voituriez, *Biophys. J.* **101**, 1041 (2011).
- [8] K. Tawada and K. Sekimoto, *J. Theor. Biol.* **150**, 193 (1991).
- [9] F. Jülicher, K. Kruse, J. Prost, and J. Joanny, *Phys. Rep.* **449**, 3 (2007).
- [10] P. Recho and L. Truskinovsky, *Phys. Rev. E* **87**, 022720 (2013).
- [11] H. Keller, A. D. Zadeh, and P. Egli, *Cell Motil. Cytoskeleton* **53**, 189 (2002).
- [12] C. Blanch-Mercader and J. Casademunt, *Phys. Rev. Lett.* **110**, 078102 (2013).
- [13] M. Mayer, M. Depken, J. S. Bois, F. Jülicher, and S. W. Grill, *Nature (London)* **467**, 617 (2010).
- [14] K. Kruse, A. Zumdick, and F. Jülicher, *Europhys. Lett.* **64**, 716 (2003); A. Ahmadi, M. C. Marchetti, and T. B. Liverpool, *Phys. Rev. E* **74**, 061913 (2006); G. Salbreux, J. Prost, and J. F. Joanny, *Phys. Rev. Lett.* **103**, 058102 (2009).
- [15] B. Perthame, *Transport Equations in Biology* (Birkhauser Verlag, Basel, 2007).
- [16] K. Kruse and F. Jülicher, *Phys. Rev. E* **67**, 051913 (2003).
- [17] V. Calvez, N. Meunier, and R. Voituriez, *C. R. Seances Acad. Sci., Ser. A* **348**, 629 (2010).
- [18] S. J. Altschuler, S. B. Angenent, Y. Wang, and L. F. Wu, *Nature (London)* **454**, 886 (2008); A. Jilkine and L. Edelstein-Keshet, *PLoS Comput. Biol.* **7**, e1001121 (2011).
- [19] K. Keren, Z. Pincus, G. M. Allen, E. L. Barnhart, G. Marriott, A. Mogilner, and J. A. Theriot, *Nature (London)* **453**, 475 (2008); A. E. Carlsson and D. Sept., *Methods Cell Biol.* **84**, 911 (2008); M. Herant and M. Dembo, *Biophys. J.* **98**, 1408 (2010); K. Doubrovinski and K. Kruse, *Eur. Phys. J. E* **31**, 95 (2010); D. Shao, W.-J. Rappel, and H. Levine, *Phys. Rev. Lett.* **105**, 108104 (2010); E. L. Barnhart, K.-C. Lee, K. Keren, A. Mogilner, J. A. Theriot, and J. B. Alberts, *PLoS Biol.* **9**, e1001059 (2011); F. Ziebert, S. Swaminathan, and I. S. Aranson, *J. R. Soc. Interface* **9**, 1084 (2012).
- [20] B. Rubinstein, M. F. Fournier, K. Jacobson, A. B. Verkhovskiy, and A. Mogilner, *Biophys. J.* **97**, 1853 (2009).
- [21] A. Callan-Jones and R. Voituriez, *New J. Phys.* **15**, 025022 (2013).
- [22] K. Kruse, J. F. Joanny, F. Jülicher, and J. Prost, *Phys. Biol.* **3**, 130 (2006).
- [23] E. L. Barnhart, G. M. Allen, F. Jülicher, and J. A. Theriot, *Biophys. J.* **98**, 933 (2010); X. Du, K. Doubrovinski, and M. Osterfield, *Biophys. J.* **102**, 1738 (2012); A. J. Loosley and J. X. Tang, *Phys. Rev. E* **86**, 031908 (2012); S. Banerjee and M. C. Marchetti, *Phys. Rev. Lett.* **109**, 108101 (2012).
- [24] E. F. Keller and L. A. Segel, *J. Theor. Biol.* **30**, 225 (1971).
- [25] E. M. Purcell, *Am. J. Phys.* **45**, 3 (1977).
- [26] E. Caglioti, P. L. Lions, C. Marchioro, and M. Pulvirenti, *Commun. Math. Phys.* **143**, 501 (1992); C. C. Chen and C. S. Lin, *Ann. Inst. H. Poincaré (C)* **18**, 271 (2001); F. Gladiali *et al.*, [arXiv:1210.1373](https://arxiv.org/abs/1210.1373).
- [27] J. Carr and R. L. Pego, *Commun. Pure Appl. Math.* **42**, 523 (1989).